

Reservoir Sedimentation Assessment Using Geospatial Technology: A Case Study of Dukan Reservoir, Sulaimani Governorate, Kurdistan Region, Iraq

Haveen Muhammed Rashid

Department of Water Resources Engineering, College of Engineering, University of Sulaimani, Sulaimai, Iraq

haveen.rashid@univsul.edu.iq

ABSTRACT

The accumulation of sediment in reservoirs poses a major challenge that impacts the storage capacity, quality of water, and efficiency of hydroelectric power generation systems. Geospatial methods, including Geographic Information Systems (GIS) and Remote Sensing (RS), were used to assess Dukan Reservoir sediment quantities. Satellite and reservoir water level data from 2010 to 2022 were used for sedimentation assessment. The satellite data was used to analyze the water spread area, employing the Normalized Difference Water Index (NDWI) and Modified Normalized Difference Water Index (MNDWI) to enhance the water surface in the satellite imagery of Dukan Reservoir. The cone formula was employed to calculate the live storage capacity of the reservoir within two elevations. According to the study results, the live storage capacity of Dukan Reservoir at elevation 511.78 m had decreased from 8000 MCM to 7007.77MCM and 6923.53 MCM using NDWI and MNDWI respectively, due to sedimentation, resulting in a capacity loss of 14.59% and 15.83% for NDWI and MNDWI respectively. The annual sedimentation was 13.78 MCM and 14.95 MCM for NDWI and MNDWI, respectively. Joglekar's equation and Khosla's formula have demonstrated that the sedimentation rate in the Dukan reservoir exceeds the critical rate. The findings of this study will inform the development of sediment management strategies aimed at preserving the reservoir's capacity.

Keywords: Elevation-Capacity curve, NDWI, MNDWI, Remote sensing technique, Sediment rate.

*Corresponding author

Peer review under the responsibility of University of Baghdad.

<https://doi.org/10.31026/j.eng.2023.12.05>

This is an open access article under the CC BY 4 license (<http://creativecommons.org/licenses/by/4.0/>).

Article received: 15/04/2023

Article accepted: 14/09/2023

Article published: 01/12/2023



تقييم ترسيب الخزان باستخدام التكنولوجيا الجيومكانية: دراسة حالة لخزان دوكان، محافظة السليمانية، إقليم كردستان، العراق

هفين محمد رشيد

قسم هندسة الموارد المائية، كلية الهندسة، جامعة السليمانية، السليمانية، العراق

الخلاصة

يشكل تراكم الرواسب في الخزانات تحديًا كبيرًا يؤثر على سعة التخزين ونوعية المياه وكفاءة أنظمة توليد الطاقة الكهرومائية. تم استخدام الأساليب الجغرافية المكانية، بما في ذلك نظم المعلومات الجغرافية (GIS) والاستشعار عن بعد (RS) في تقييم كميات الرواسب في خزان دوكان. تم استخدام بيانات الأقمار الصناعية وبيانات منسوب مياه الخزان من عام 2010 إلى عام 2022 لإجراء تقييم الترسيب. تم استخدام بيانات القمر الصناعي لتحليل منطقة انتشار المياه، باستخدام مؤشر ماء الفروق الطبيعي (NDWI) ومؤشر ماء الفروق المعياري المعدل (MNDWI) لتحسين سطح الماء في صور القمر الصناعي لخزان دوكان. لحساب سعة التخزين الحية للخزان على ارتفاعين، تم استخدام الصيغة المخروطية. وفقًا لنتائج الدراسة، انخفضت السعة التخزينية الحية لخزان دوكان على ارتفاع 511.78 مترًا من 8000 مليون متر مكعب إلى 7007.77 مليون متر مكعب و 6923.53 مليون متر مكعب باستخدام NDWI و MNDWI على التوالي، بسبب الترسيب، مما أدى إلى فقدان السعة بنسبة 14.59% و 15.83% لـ NDWI و MNDWI على التوالي. بلغ الترسيب السنوي 13.78 مليون متر مكعب و 14.95 مليون متر مكعب باستخدام NDWI و MNDWI على التوالي. أثبتت معادلة جوجلكار وصيغة خوسلا أن معدل الترسيب في خزان دوكان يتجاوز المعدل الحرج. ستفيد نتائج هذه الدراسة في تطوير استراتيجيات إدارة الرواسب التي تهدف إلى الحفاظ على سعة الخزان.

الكلمات المفتاحية: منحني قدرة الارتفاع، NDWI، MNDWI، تقنية الاستشعار عن بعد، معدل الرواسب.

1. INTRODUCTION

Reservoir sedimentation is the accumulation of sediment, such as sand, silt, and clay, in a reservoir created by a dam. Sedimentation in reservoirs is a natural process due to land erosion and sediment transportation by rivers and streams (Li et al., 2018; Bhattacharyya and Singh, 2019; Ren et al., 2021). Several factors contribute to accelerated sediment erosion and deposition into streams and rivers. These factors include deforestation, changes in vegetation cover, topography, climate change, grazing practices, inappropriate tillage techniques, unsustainable agricultural practices, and anthropogenic land use practices (Amore et al., 2004; Dadoria et al., 2017).

It is noted that the important task is the assessment of sediment in reservoirs since the sediment buildup can reduce the reservoir storage capacity, affect the productivity and efficiency of hydroelectric power plants, and alter water quality (Ali et al., 2020). Different approaches can be used to estimate reservoir sedimentation: acoustic doppler current profile, side-scan sonar, particle tracking, sediment trap monitoring, radiometric dating, bathymetric survey, and remote sensing (Gao, 2009; Liu et al., 2022). The remote sensing approach utilizes aerial imagery to assess changes in the reservoir's



water level, denoting sediment buildup. Furthermore, this method permits the estimation of sediment capacity in the reservoir by analyzing the water's color and reflectance features.

Combining GIS and remote sensing methods presents an important mechanism for estimating reservoir sediment. By merging data from various sources, including satellite imagery, on-site surveys, and sediment patterns, assessment of sediment reservoirs can be achieved. This can aid reservoir administrators to make more informed choices about sediment management strategies, such as dredging or sediment extraction (**Afshar et al., 2016; Aziz et al., 2021**). Besides its advantages, there are some limitations to using satellite remote sensing for reservoir estimation, including capacity estimation using remote sensing can only be done between the full reservoir level (FRL) and the minimum water level in the reservoir (**Vishwakarma et al., 2015; Shendge and Chockalingam, 2016**). A lack of cloud-free dates throughout the reservoir operation period can pose a challenge. Remote sensing techniques provide accurate estimations for fan-shaped reservoirs with a considerable change in water-spread area for incremental changes in water level. The accuracy of the assessment can be impacted by the potential occurrence of errors in identifying the tail end of the reservoir.

The global estimate for reservoir sedimentation rates varies widely depending on various factors, such as the size and location of the reservoir, watershed characteristics, climate, land use practices, and sedimentation management strategies. Based on the research conducted by (**White, 2001; Pandey et al., 2016; Merina et al., 2016; Ali et al., 2020; CIGB, I., 2023**), the global average annual sedimentation rate for reservoirs is assessed within the range of 0.5-1% of the reservoir volume, which can lead to considerable decreases in the storage capacity of the reservoir over time. Nevertheless, sedimentation rates can vary extremely, with certain reservoirs undergoing elevated sedimentation rates, especially in areas with increased soil corrosion rates or high sediment loads in rivers. Several studies have been undertaken to estimate reservoir sedimentation, utilizing remote sensing methods like satellite imagery, aerial photography, and LiDAR. These approaches have demonstrated effective mechanisms for recognizing changes in reservoir sedimentation over time, especially in larger reservoirs. The upcoming literature review summarizes the research conducted in this field.

(Pandey et al., 2016) applied remote sensing techniques to assess the sedimentation in Patratu Reservoir. The reservoir receives an average inflow of 101.95 hm³ per year. The initial designed sedimentation rate for the Patratu reservoir was 11.73 ha-m/year, with a trapping efficiency of 96%. The researchers utilized data on water levels and satellite imagery from 2006 to 2012 and calculated the water spread area to evaluate sedimentation. Their findings indicated that sedimentation caused a decrease in the live storage capacity of the Patratu reservoir from 101.95 hm³ to 89.96 hm³, resulting in a capacity loss of 11.76% over 44 years. A research investigation was carried out by **(Dewangan and Ahmad, 2020)**, in which RS and GIS techniques were utilized to evaluate the sediment accumulation in the Kodar River watershed's reservoir. Landsat – 8 imagery was employed in the study to estimate the reservoir's capacity at different elevations. The study findings reveal that over 36 years, sedimentation has resulted in a loss of 14.39% of the reservoir's capacity. Moreover, the average rate of soil erosion is calculated to be 5.50 tons/hectare.year. **(Nijampurkar et al., 2020)** conducted research involving using RS and GIS techniques and analyzing Landsat-8 images to evaluate the water diffusion zone of Morbe dam at various heights in 2007. They employed the linear interpolation/extrapolation method to estimate the capacity loss of the dam from 2007



to 2018 by comparing the revised reservoir capacity calculated using the Prizmoidal formula with the initial capacity in 2007. Based on the results, the live storage capacity was reduced from 190.89 MCM to 186.251 MCM, signifying a total capacity loss of 4.6390 MCM or 2.4302% over eleven years. Furthermore, they evaluated that the sedimentation progress in a linear fashion would produce an annual sedimentation rate of 0.4217 MCM. **(Iradukunda and Bwambale, 2021)** conducted a study to assess sedimentation and its effect on storage loss in the Murera reservoir. According to their findings, the reservoir increased in depth from its northern to southern locations, accessing a maximum depth of 7.78 m. Additionally, the total water storage capacity of the reservoir reached 707,862 m³. The findings also indicated that sediment deposition was notably lower in the northern part of the reservoir than in the southern part. **(Singh et al., 2023)** calculated the reduction in live storage in the Samrat Ashok Sagar reservoir caused by sedimentation using satellite imagery. The study utilized satellite images from seven dates and analyzed the reservoir's live storage elevation data obtained from field records using ArcGIS software. The study's findings indicate that sedimentation in the live storage area of the reservoir amounted to around 46.48 MCM over 20 years from 1997 to 2017, with an annual sedimentation rate of 2.324 MCM or 0.9% per year.

Several studies investigate the sedimentation rate, sediment transport, and deposition in Dukan Reservoir using various methods such as numerical modeling, GIS analysis, and sediment transport modeling. Some are presented below:

In their study, **(Hassan et al., 2016)** conducted a field survey and analyzed the grain size of sediment samples collected from 32 locations across the entire area of the Dukan reservoir. The reservoir was formed in 1959 by damming the Lesser Zab River. The researchers collected thirty-two samples from the reservoir bed, consisting of 23% clay, 48% silt, 14% sand, and 15% gravel. **(Hassan et al., 2017)** carried out a bathymetric survey over 10 days in November 2014 using a single-beam echo sounder. According to the survey results, the average amount of sediment deposition per year was 3.8 MCM. The researchers collected 32 sediment samples from the reservoir bed and found that the gravel, sand, silt, and clay had a ratio of 15:14:48:23, respectively. Silt mostly covers the reservoir bed, with the sediment composition being 77.6% silty clay, 10% silty sandy clay, 1.2% sandy gravely silty clay, and 1% gravely sandy silty clay. In a study by **(Ezz-Aldeen et al., 2018)**, the researchers used the soil and water assessment tool (SWAT) model to evaluate the annual runoff and sediment loads of the Dukan Dam watershed. The aim was to determine the contributions of the watershed and Lesser Zab River compared to the total values and identify basins with a high sediment load per unit area. While calibrating between 1961 and 1968, the researchers assessed statistical measures like coefficient of determination and Nash-Sutcliffe model efficiency. They determined the Nash-Sutcliffe model efficiency and coefficient of determination for runoff to be 0.64 and 0.75, respectively, and for sediment load to be 0.63 and 0.65, according to a study conducted by **(Ali et al., 2020)**. Based on a bathymetric survey conducted in 2014, a new operational curve was developed for the reservoir. The reduction in reservoir capacity between 1959 and 2014 was calculated by comparing the storage capacity designed with the capacity determined from the 2014 survey. The study found that sedimentation had caused the dam's capacity to decrease by 25%, which corresponds to an estimated volume of 367 MCM at a water level of 480 meters. It was found that the yearly sedimentation rate amounted to approximately 6.6 MCM, while the estimated sediment yield was 701.2 tons per cubic kilometre per year. **(Jameel et al., 2022)** examined the efficiency of trapping sediment in the Dukan reservoir using ResCon 2.2. The study found



that sediment siltation occurs at a rate of 3.8 MCM per year and that multiple factors, such as the reservoir's shape behind the dam, rate of sedimentation, trap efficiency (TE), and sediment management process, must be identified for accurate reservoir sedimentation analysis. Different methods of sediment management to forecast Dukan dams trap efficiency for up to 300 years during the project's lifespan. Data analysis revealed that the dam's TE would remain at 97% until 2055. The ResCon 2.2 model was utilized to identify the most efficient sediment management techniques, and the study found that catchment management, by-pass, and trucking yielded TE values of approximately 95%, 96%, and 97%, respectively.

Dukan Reservoir is facing concerns about the potential impact of climate change, with experts warning of the possibility of increased droughts and decreased rainfall. Additionally, the varying effects of flood and flush rainfall on reservoir sedimentation could negatively affect agriculture, electricity generation, and local communities. A current study utilizes a remote sensing approach to determine the range of reservoir capacity loss due to sedimentation.

2. MATERIALS AND METHODS

2.1 Study Area Description

The study area is located in the northwestern part of Sulaimani Governorate, about 65 km from the city center (**Sreepada et al., 2018; Jameel et al., 2022**). It is located in the Lesser Zab River, which encompasses a total area of 19780 km², with 24% situated in Iran and the remaining 76% in Iraq (**Al-Ansari and Knutsson, 2011; Al-Ansari, 2013; Al-Ansari et al., 2014; Al-Ansari et al., 2015**). The extremities of the lake extended from East between longitude 44° 45'- 45° 03' and from North between latitude 35° 57'- 36° 14' as in **Fig. 1**. Information of Dukan reservoir and its hydrological features is shown in **Table 1**.

Table 1. Description of Dukan reservoir and related hydrology aspects (**Othman, 2016**)

Reservoir	
Capacity at elevation 511m	6800M m ³
Active Capacity	6100M m ³
Dead Storage Volume	700M m ³
Surface area at level 511 m	270 km ²
Maximum elevation	515 m
Normal elevation	511 m
Minimum drawdown level	469 m
Hydrology	
Catchment Area	11690 km ²
Mean annual precipitation	850 mm

The Dukan Reservoir is one of the largest bodies of water in Iraq. It is a major hydroelectric power source, with the Dukan Dam generating up to 1,000 Megawatts of electricity. In addition to its importance as a power source, the Dukan Reservoir provides irrigation water for agriculture and is a popular destination for recreational activities

such as boating and fishing. The surrounding area is known for its scenic beauty, with the lake's clear blue waters and rugged mountainous terrain attracting many visitors. The reservoir consists of two distinct reservoirs. The larger of the two is located in the northern section of a nearly triangular basin, as depicted in **Fig. 2**. The triangle base measures up to 16 km. In comparison, the hypotenuse has a length of approximately 20.5 km. On the other hand, the smaller reservoir has an approximate square shape, measuring 3 km in length and 4 km in width (**Ali et al., 2020**).

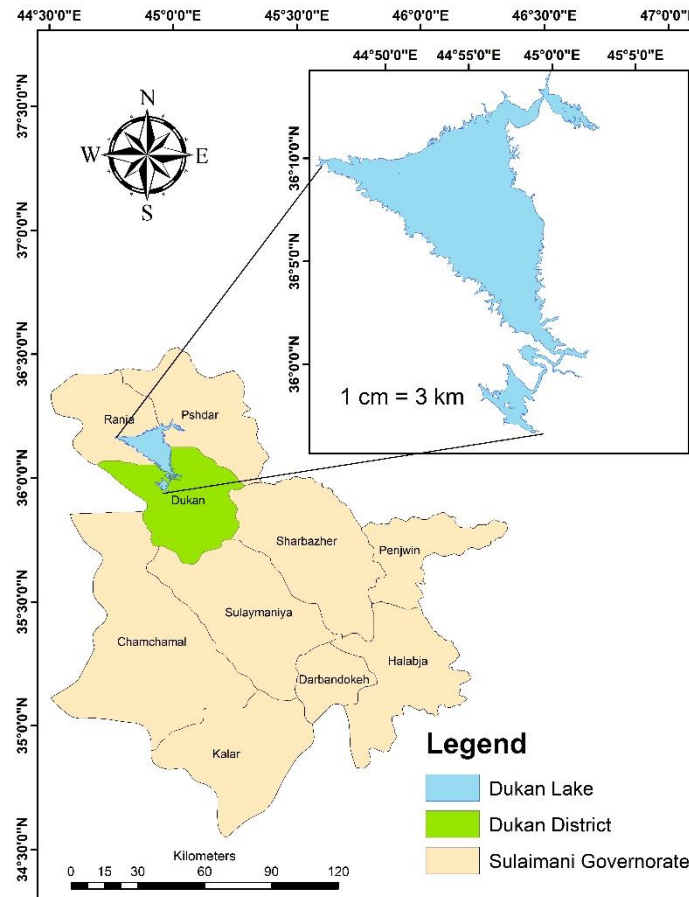


Figure 1. Study Area Location

2.2 Data Used

Considering the different reservoir levels between minimum draw down and full reservoir levels on various dates between 2010 and 2022. The sedimentation study focused on this period because it was noted to have the greatest elevation difference recorded, ranging from 478.39 to 511.78m. Ten Landsat images have been selected for analysis. Nine of these images were acquired from Landsat 8 OLI/TIRS (Path 169, Row 35), while one image was obtained from Landsat 5 TM/C2 L1 (Path 168, Row 35). These images were obtained from Global Visualization (GloVis) Viewer (**USGS, 2005**) with a resolution of 30mx30m and projected coordinate system WGS84_UTM Zone 38N. The satellite data used in the analysis is shown in **Table 2**. The water level for the same date of the satellite pass was acquired from the Dukan Dam Directorate.

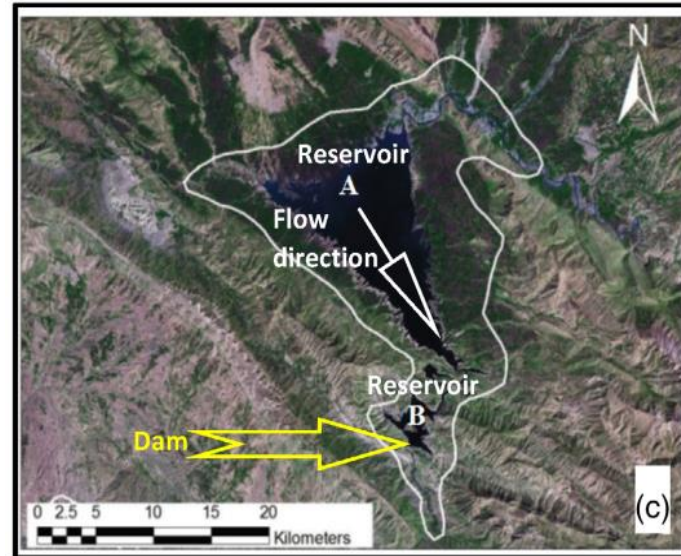


Figure 2. Dukan upper and lower reservoir (Ali et al., 2020)

Table 2. Detail of Data Used

Date of Satellite Pass	Satellite	Path	Row	Water level [m]
25 Dec 2010	Landsat 5 TM/C2 L1	168	35	478.39
15 Nov 2022	Landsat 8 OLI/TIRS	169	35	488.68
16 Feb 2016	Landsat 8 OLI/TIRS	169	35	493.12
19 Mar 2016	Landsat 8 OLI/TIRS	169	35	496.81
31 Jul 2018	Landsat 8 OLI/TIRS	169	35	499.29
20 Jul 2020	Landsat 8 OLI/TIRS	169	35	502.42
25 May 2017	Landsat 8 OLI/TIRS	169	35	503.35
24 Feb 2019	Landsat 8 OLI/TIRS	169	35	506.05
31 May 2019	Landsat 8 OLI/TIRS	169	35	510.69
13 Apr 2019	Landsat 8 OLI/TIRS	169	35	511.78

2.3 Estimation of Water Spread Area

The fundamental concept behind utilizing Satellite Remote Sensing to assess reservoir sedimentation involves determining the water-covered surface area of the reservoir using satellite data for different water levels ranging from minimum draw-down level to full reservoir level. Remote sensing technology is used to collect satellite images with the required spectral bands, which are then processed using ArcGIS version 10.5 to extract the spectral information needed to calculate the Normalized Difference Water Index (NDWI) and Modified Normalized Difference Water Index (MNDWI). These indices are used to delineate water bodies from surrounding land areas, as water bodies have high reflectance in the respective spectral bands (Kumar et al., 2013; Dadoria et al., 2017; Singh et al., 2023; Kodimela et al., 2023).

Once the NDWI and MNDWI values are calculated for each pixel in the image, the results are displayed using color scales, with water bodies appearing blue or dark. In contrast, non-water areas appear in other colors depending on their reflectance values. NDWI is



calculated using the green and near-infrared (NIR) bands, while MNDWI uses the green and short-infrared (SWIR) bands. NDWI and MNDWI can be calculated using the following formulas:

$$NDWI = \frac{(Green-NIR)}{(Green+NIR)} \quad (1)$$

$$\text{For Landsat 8 data, } NDWI = \frac{(Band\ 3-Band\ 5)}{(Band\ 3+Band\ 5)} \quad (2)$$

Nevertheless, the outturn produced by the formula mentioned above is of low precision, as clarified water does not reflect in either NIR or SWIR. To solve this limitation, **(Xu, 2005)** established enhancements to the NDWI formula by including the Green and SWIR bands, leading to an upgraded assessment method.

$$MNDWI = \frac{(Green-SWIR)}{(Green+SWIR)} \quad (3)$$

$$\text{For Landsat 8 data, } MNDWI = \frac{(Band\ 3-Band\ 6)}{(Band\ 3+Band\ 6)} \quad (4)$$

In the above formulas, Green, NIR, and SWIR show the values of the particular spectral bands. Both indices' values range from -1 to 1, with water bodies generally producing values more than 0.5. Conversely, vegetation produces significantly lower values, making it easily distinguishable from water bodies. Positive values between 0 and 0.2 are observed in built-up features **(Husain, 2016; Priyanka et al., 2017)**. **Fig. 3** displays the water spread area obtained from all the satellite images using NDWI. The area was at its lowest in the year 2010 and peaked in the year 2019.

2.4 Estimation of Reservoir Capacity

To assess the capacity of a reservoir, the cone equation is utilized, taking into account input variables such as water spread areas acquired from remote sensing data and height data calculated by comparing two consecutive reservoir levels **(Singh et al., 2023; Avinash and Chandramouli, 2018)**. The original elevation-area and elevation-capacity curves were first carried out in 1950, before the dam's construction, and were obtained from **(Binnie and Partners, 1987; Hassan et al., 2017; Ali et al., 2020)**. The sedimentation rate can be determined by comparing the original elevation-capacity curve with the cumulative capacity obtained through remote sensing.

Listed below is the cone equation used for calculating the storage capacity of a reservoir between two distinct water levels.

$$V_{1-2} = \frac{\Delta h(A_1+A_2+\sqrt{A_1 \cdot A_2})}{3} \quad (5)$$

where V_{1-2} is the Volume between levels 1 and 2 consecutively

A_1 and A_2 - Reservoir water area at levels 1 and 2

Δh - elevation change between levels 1 and 2

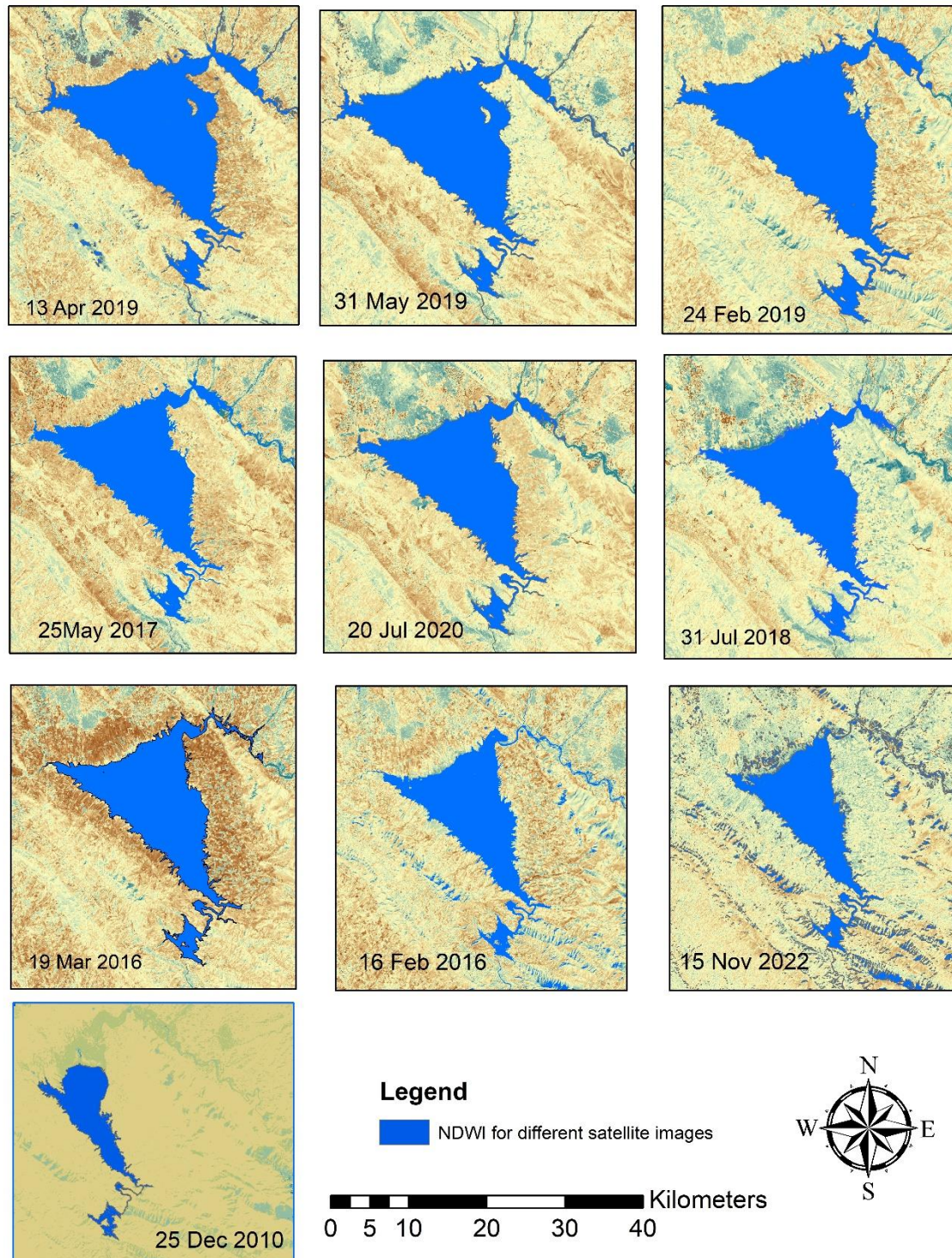


Figure 3. Water spread area using NDWI for the selected satellite date pass

The revised elevation-area and elevation-capacity curves are shown in **Figs. 4 and 5**. The detailed calculation of reservoir cumulative capacity using NDWI and MNDWI are shown in **Tables 3 and 4**, respectively.

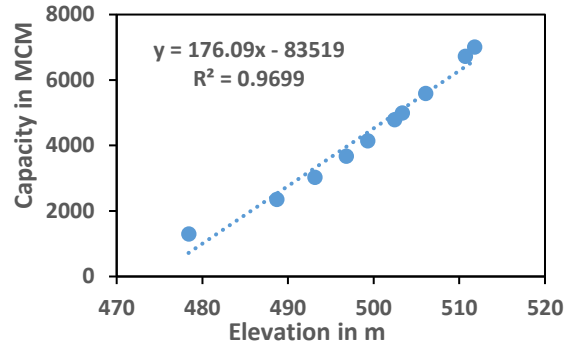
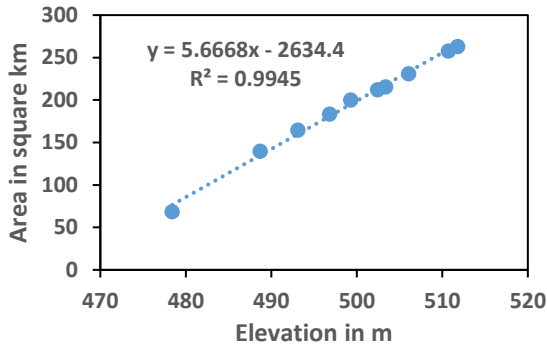


Figure 4. Elev.-Area curve using NDWI

Figure 5. Elev.-Capacity curve using NDWI

The sedimentation rate obtained through remote sensing methods was then compared to Khosla's formula and Joglekar's equation (Subramanya, 2008). The Khosla's formula and Joglekar's equation may be written as:

Khosla's formula:

$$Q_s = \frac{0.323}{A^{0.28}} \tag{6}$$

Joglekar's equation:

$$Q_s = \frac{0.597}{A^{0.24}} \tag{7}$$

Q_s represents the yearly sediment accumulation rate ($Mm^3/100 \text{ km}^2/\text{year}$) for a watershed area of 100 km^2 , while A refers to the total catchment area measured in km^2 .

Table 3. Estimation of reservoir capacity using NDWI

Date	Elevation (m)	NDWI (km^2)	Head difference	Volume (MCM)	Accumulated Volume	Volume 1950	Volume difference
25-Dec-10	478.39	68.41	0	1300	1300	1400	100
15-Nov-22	488.68	139.85	10.29	1049.80	2349.80	3299	949.20
16-Feb-16	493.12	164.67	4.44	675.28	3025.09	3161.2	136.11
19-Mar-16	496.81	183.71	3.69	642.44	3667.53	3947	279.47
31-Jul-18	499.29	200.02	2.48	475.68	4143.21	4578	434.79
20-Jul-20	502.42	212.37	3.13	645.29	4788.50	5514.5	726.00
25-May-17	503.35	215.59	0.93	199.00	4987.50	5827	839.50
24-Feb-19	506.05	231.054	2.7	602.85	5590.35	6833	1242.65
31-May-19	510.69	257.82	4.64	1133.61	6723.97	7500	776.03
13-Apr-19	511.78	262.933	1.09	283.80	7007.77	8000	992.23



Table 4. Estimation of reservoir capacity using MNDWI

Date	Elevation (m)	MNDWI (km ²)	Head difference	Volume (MCM)	Accumulated Volume	Volume 1950	Volume difference
25-Dec-10	478.39	68.1	0	1300.00	1300	1400	100.00
15-Nov-22	488.68	135.05	10.29	1025.74	2325.74	3299	973.26
16-Feb-16	493.12	159.86	4.44	653.92	2979.66	3161.2	181.54
19-Mar-16	496.81	180.66	3.69	627.86	3607.53	3947	339.47
31-Jul-18	499.29	199.53	2.48	471.24	4078.77	4578	499.23
20-Jul-20	502.42	210.55	3.13	641.70	4720.47	5514.5	794.03
25-May-17	503.35	214.31	0.93	197.56	4918.03	5827	908.97
24-Feb-19	506.05	230.89	2.7	600.88	5518.90	6833	1314.10
31-May-19	510.69	253.92	4.64	1124.33	6643.23	7500	856.77
13-Apr-19	511.78	260.40	1.09	280.30	6923.53	8000	1076.47

3. RESULTS AND DISCUSSION

The updated cumulative capacity of water between the selected highest level of 511.78m and the available lowest level of 478.39m was calculated as shown in Fig. 6. It was determined that the capacity of the reservoir had decreased by 992.23 MCM and 1076.47MCM at elevation 511.78m for NDWI and MNDWI respectively due to sedimentation, resulting in a capacity loss of 14.59% and 15.83% for NDWI and MNDWI respectively over 72 years. The satellite remote sensing survey indicated an annual sedimentation rate of 13.78 MCM and 14.95 MCM for NDWI and MNDWI, respectively. In addition, the yearly sedimentation rates for NDWI and MNDWI were 0.2% and 0.22%, respectively, within the standard annual reservoir sediment percentage range of 1% (Ali et al., 2020).

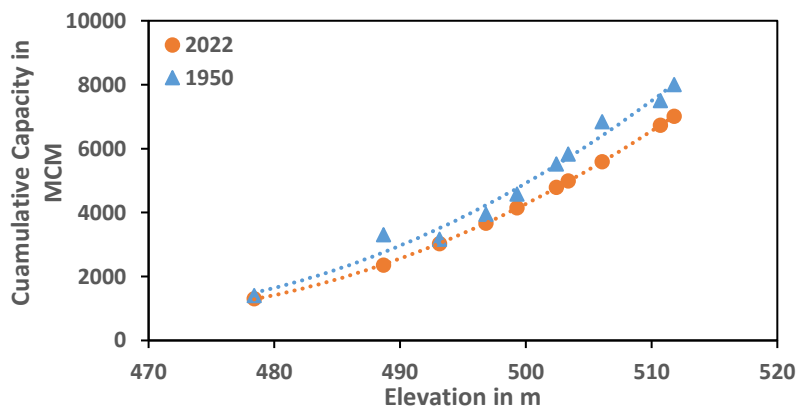


Figure 6. Revised Elev. Capacity curve using NDWI and Original curve in 1950

The reservoir area obtained using NDWI varied from 68.41 to 262.93 km², with the lowest value recorded on December 25, 2010, and the highest on April 13, 2019. On the other hand, when using MNDWI, the reservoir area ranged from 68.1 to 260.4 km², with the minimum value in 2010 and the maximum value in 2019. On average, there was a difference of 2.54 km² in areas calculated between NDWI and MNDWI, with the use of MNDWI resulting in an average reduction in the area of approximately 1.4 % and an increase in sedimentation rate of 8.5%. Both indices determined the water spread areas. However, the NDWI-derived image had less prominent water features compared to the



MNDWI-derived image. This was because of negative NDWI values and the water blending with built-up features. On the other hand, the MNDWI index yielded more enhanced water features, as the values were positive for water features mixed with vegetation. In addition, the study highlights that remote sensing-based estimation of sedimentation is greatly influenced by the accuracy of water-spread area determination, water level data, and the original elevation-area-capacity table.

As the catchment area of Dukan dam is 11690 km², the annual rate of sedimentation has been calculated using Joglekar's equation and Khosla's formula, resulting in values of 0.063 MCM/100km² and 0.0234 MCM/100km² respectively. However, the study has found that the annual sedimentation rate was 0.12 MCM/100 km², and 0.128 MCM/100 km² for NDWI and MNDWI, respectively. Therefore, both the formulas mentioned above underestimate the rate of siltation compared to the founded results. Hence, it is imperative to implement effective soil conservation techniques within the watershed area to minimize the erosion and sedimentation that could enter the Dukan Dam.

4. CONCLUSIONS

Conventional hydrographic surveys, though effective, are notorious for being time-consuming, labor-intensive, and costly. However, remote sensing techniques provide a cost-effective and efficient option for estimating capacity loss. According to the results of the satellite remote sensing conducted on Dukan reservoir, it was discovered that the reservoir's live storage capacity had decreased from its original capacity of 8000 MCM to 7007.77MCM and 6923.53 MCM at elevation 511.78 m, indicating 14.59% and 15.83% reduction for NDWI and MNDWI respectively. The range of variation in the reservoir's water level determines the sedimentation rate. If the sedimentation rate for the entire reservoir needs to be determined, hydrographic surveys may be performed within the water-spread area corresponding to the lowest recorded elevation in addition to analyzing remote sensing data. Joglekar's equation and Khosla's formula, among other empirical formulas, have demonstrated that reservoir sedimentation rates exceed the critical rate. To maintain the carrying capacity and cleanliness of the lake, corrective measures should be taken regularly, including prohibiting illegal fishing activities, establishing buffer zones, discontinuing the release of excessive pollutants from agricultural zones, and removing weeds and silt from the reservoir.

ACKNOWLEDGMENTS

The author expresses gratitude to (Mr. Kochar Jamal Tawfeeq) director of Dukan Dam, for providing the observed water level data used in the current work.

NOMENCLATURE

Symbol	Description	Symbol	Description
A	Total catchment area measured in km ² or Reservoir water area	V1-2	Volume between levels 1 and 2 consecutively
A1,A2	Reservoir water area at levels 1 and 2	Δh	elevation change between levels 1 and 2
Qs	yearly sediment accumulation rate (Mm ³ /100 km ² /year)	MNDWI	Modified Normalized Difference Water Index



REFERENCES

- Afshar, S., Shamasai, A., and Saghafian, B., 2016. Dam sediment tracking using spectrometry and Landsat 8 satellite image, Taleghan Basin, Iran. *Environmental Monitoring and Assessment*, 188(104). [Doi:10.1007/s10661-015-5052-y](https://doi.org/10.1007/s10661-015-5052-y).
- Al-Ansari, N., 2013. Management of water resources in Iraq, Perspectives and prognoses. *Engineering*, 5(8), pp. 667-684. [Doi:10.4236/eng.2013.58080](https://doi.org/10.4236/eng.2013.58080).
- Al-Ansari, N., 2013. Management of water resources in Iraq: perspectives and prognoses. *Engineering*, 5(6), pp. 667-684.
- Al-Ansari, N., Ali, A., and Knutsson, S., 2014. Present conditions and future challenges of water resources problems in Iraq. *Journal of Water Resources and Protection*, 6, pp. 1066-98. [Doi:10.4236/jwarp.2014.612102](https://doi.org/10.4236/jwarp.2014.612102).
- Al-Ansari, N., Ali, A., and Knutsson, S., 2015. Iraq water resources planning: perspectives and prognoses. Jeddah, Saudi Arabia, pp. 2097-2108.
- Al-Ansari, N., and Knutsson, S., 2011. Toward prudent management of water resources in Iraq. *Journal of Advanced Science and Engineering Research*, 1, pp. 53-67. [Doi:10.4236/jss.2016.43010](https://doi.org/10.4236/jss.2016.43010).
- Ali A., Hassan, R., Hazim, A., Al-Ansari, Ali, S., and Knutsson, S., 2020. Sediment flux from Lesser Zab River in Dokan Reservoir: Implications for the sustainability of long-term water resources in Iraq, River Research application. *River Research and Applications*, 1(11), pp. 351-361. [Doi:10.1002/rra.3595](https://doi.org/10.1002/rra.3595).
- Amore, E., Modica, C., Nearing, M.A., and Santoro, V.C., 2004. Scale effect in USLE and WEPP application for soil erosion computation from three Sicilian basins. *Journal of Hydrology*, 293, pp. 100-114. [Doi:10.1016/j.jhydrol.2004.01.018](https://doi.org/10.1016/j.jhydrol.2004.01.018)
- Avinash, G., and Chandramouli, P., 2018. Assessment of reservoir sedimentation using RS and GIS techniques -A case study of Kabini Reservoir, Karnataka, India. *International Research Journal of Engineering and Technology*, 5(8), pp. 630-635.
- Aziz, A., Essam, Y., Ahmed, A., Huang, Y., and El-Shafie, A., 2021. An assessment of sedimentation in Terengganu River, Malaysia using satellite imagery. *Ain Shams Engineering Journal*, 12(4), pp. 3429-3438. [Doi:10.1016/j.asej.2021.03.014](https://doi.org/10.1016/j.asej.2021.03.014)
- Bhattacharyya, K., and Singh, V., 2019. Reservoir sedimentation. Assessment and environmental controls. CRC Press.
- Binnie and Partners, 1987. Analysis and Safety Evaluation of Dokan Dam. (Overseas) Ltd., Final Report, 1.
- Dadoria, D., Tiwari, H., and Jaiswal, R., 2017. Assessment of reservoir sedimentation in Chhattisgarh state using remote sensing and GIS. *International Journal of Civil Engineering and technology*, 8(4), pp. 526-534.
- Dewangan, C., and Ahmad, I., 2020. Assessment of reservoir sedimentation and identification of critical soil erosion zone in Kodar reservoir watershed of Chhattisgarh state, India. In: *Applications in Gematics in Civil Engineering. Select Proceedings of ICGCE 2018*. (pp. 203-214). [Doi:10.1007/978-981-13-7067-0_16](https://doi.org/10.1007/978-981-13-7067-0_16).



- Ezz-Aldeen, M., Hassan, R., Ali, A., Al-Ansari, N., and Knutsson, S., 2018. Watershed sediment and its effect on storage capacity: Case study of Dokan Dam Reservoir. *Water*, 10(7), p.858. [Doi:10.3390/w10070858](https://doi.org/10.3390/w10070858)
- Gao, J., 2009. Bathymetric mapping by means of remote sensing: Methods, accuracy and limitations. *Progress in physical geography*, 33(1), pp. 103-116. [Doi:10.1177/0309133309105657](https://doi.org/10.1177/0309133309105657).
- Hassan, R., Al-ansari, N., Ali, A., ali, S., and Knutsson, S., 2017. Bathymetry and siltation rate for Dokan reservoir, Iraq. *Lakes and Reservoirs: Research and Management*, 20(2), pp. 1-11. [Doi:10.1111/lre.12173](https://doi.org/10.1111/lre.12173)
- Hassan, R., Al-Ansari, N., Ali, S., Ali, A., Abdulla, T., and Knutsson, S., 2016. Dukan dam reservoir bed sediment, Kurdistan region, Iraq. *Engineering*, 8, pp. 582-596. [Doi:10.4236/eng.2016.89054](https://doi.org/10.4236/eng.2016.89054)
- Husain, Y., 2016. Monitoring and calculating the surface area of lakes in northern Iraq using satellite images. *Applied Research Journal*, 2(2), pp. 54-62.
- CIGB, I., 2023. Sedimentation and sustainable use of reservoirs and river systems (1st ed.). CRC Press. [Doi:10.1201/9781003316428](https://doi.org/10.1201/9781003316428)
- Iradukunda, P., and Bwambale, E., 2021. Reservoir sedimentation and its effect on storage capacity–A case study of Murera reservoir, Kenya, P., *Cogent Engineering*, 8. [Doi:10.1080/23311916.2021.1917329](https://doi.org/10.1080/23311916.2021.1917329)
- Jameel, M., Shemal, K., Sen, S., and Perumal, M., 2022. Assessment of trap efficiency of Dokan dam with different sediment management techniques using ResCon 2.2., IOP Conf. Ser.: Earth Environ. Sci., 1120. [Doi:10.1088/1755-1315/1120/1/012041](https://doi.org/10.1088/1755-1315/1120/1/012041)
- Kodimela, A., Sivaprakasam, S., and Parupally, P., 2023. Soil Loss and reservoir sedimentation assessment of Kaddam watershed using Geographical Information systems and Remote sensing Techniques. *Research square*, pp. 1-30. [Doi:10.21203/rs.3.rs-2408470/v1](https://doi.org/10.21203/rs.3.rs-2408470/v1)
- Kumar, P., Saxena, K., Tyagi, B., Nayak, A., Pandey, N., Haldar, R., and Mahanta, P., 2013. Remote sensing study on geomorphological degradation of Sarda Sagar reservoir. *Journal of Environmental Biology*, 34(6), pp. 1065-1068.
- Li, D., Lu, X., Yang, X., Chen, L., and Lin, L., 2018. Sediment load responses to climate variation and cascade reservoirs in the Yangtze river: A case study of the Jinsha river. *Geomorphology*, 322, pp. 41-52. [Doi:10.1016/j.geomorph.2018.08.038](https://doi.org/10.1016/j.geomorph.2018.08.038)
- Liu, S., Li, D., Liu, D., Znag, X., and Wang, Z., 2022. Characteristics of sedimentation and sediment trapping efficiency in the three Gorges reservoir, China. *Catena*, 208. [Doi:10.1016/j.catena.2021.105715](https://doi.org/10.1016/j.catena.2021.105715)
- Merina, N., Sashikkumar, M., Rizvana, N., and Adlin, R., 2016. Sedimentation study in a reservoir using Remote sensing Technique. *Applied Ecology and Environment*, 14(4), pp. 296-304. [Doi:10.15666/aeer/1404_296304](https://doi.org/10.15666/aeer/1404_296304)
- Nijampurkar, T., Narwade, R., and Nagarajan, K., 2020. Analysis of sedimentation deposition in Morbe reservoir by using RS and GIS. *Remote Sensing & GIS*, 11(1), P. 1624. [Doi:10.37591/v11i1.813](https://doi.org/10.37591/v11i1.813)
- Othman, L., 2016. Simulation-optimization model for Dokan reservoir system operation. MSc.Thesis.University of Sulaimani.



- Pandey, A., Chaube, U., Mishra, S., and Kumar, D., 2016. Assessment of reservoir sedimentation using remote sensing and recommendations for desilting Patratu reservoir, India. *Hydrological Sciences Journal*, 61(4), pp. 711-718. [Doi:10.1080/02626667.2014.993988](https://doi.org/10.1080/02626667.2014.993988)
- Priyanka, M., Vijaya, K., and Kanigolla, A., 2017. Assessment of Silt Deposition in Thatipudi Reservoir, Vijayanagaram District -A Geospatial Approach. *VFSTR Journal of STEM*, 3(1), pp. 2455-2462.
- Ren, S., Zhang, B., Wang, W., Yuan, Y., and Guo, C., 2021. Sedimentation and its response to management strategies of the three Gorges reservoir, Yangtze River, China. *Catena*, 199, P.105096. [Doi:10.1016/j.catena.2020.105096](https://doi.org/10.1016/j.catena.2020.105096)
- Shendge, R., and Chockalingam, M., 2016. Review of reservoir sedimentation, remote sensing and GIS technology. *International Journal of Innovations in Engineering Research and Technology*, 3(6), pp. 45-51.
- Singh, S., Prasad, B., and Tiwari, H., 2023. Sedimentation analysis for a reservoir using remote sensing and GIS techniques. *ISH Journal of Hydraulic Engineering*, 29(1), pp. 71-79. [Doi:10.1080/09715010.2021.1975318](https://doi.org/10.1080/09715010.2021.1975318)
- Sreepada, S., Munir, S., and Najmadin J., S., 2018. Optimizing reservoir operation – a case study of Dokan reservoir, Kurdistan. *ZANCO Journal of Pure and Applied Sciences*, 30, pp. 159-167.
- Subramanya, K., 2008. *Engineering Hydrology*. 3rd ed. New Delhi: McGraw-Hill.
- Nijampurkar, T., Narwade, R., and Nagarajan, K., 2020. Analysis of sedimentation deposition in morbe reservoir by using RS and GIS. *Journal of Remote Sensing*, pp. 16-24. [Doi:10.37591/v11i1.813](https://doi.org/10.37591/v11i1.813)
- USGS, 2005. *Glovis*. <https://glovis.usgs.gov/app?fullscreen=1>
- Vishwakarma, Y., Tiwari, H., and Jaiswal, R., 2015. Assessment of reservoir sedimentation using remote sensing technique with GIS model- A review. *International Journal of Engineering and Management Research*, 5(3), pp. 411-417.
- White, R., 2001. *Evacuation of sediments from reservoirs*. London, U. K.: Thomas Telfors, pp. 131-139.
- Xu, H., 2005. A Study on information extraction of water body with the Modified Normalized Difference Water Index (MNDWI). *Journal of remote sensing*, 9, pp. 589-595.
- Zhang, J., Shang, Y., Liu, J., Fu, J., Wei, S., and Tong, L., 2020. Causes of variations in sediment yield in the Jinghe river basin, China. *Scientific Reports*, 10(1), P. 18054. [Doi:10.1038/s41598-020-74980-3](https://doi.org/10.1038/s41598-020-74980-3)